Eidgenössisches Institut für Schnee- und Lawinenforschung
Institut fédéral pour l'étude de la neige et des avalanches
Istituto federale per lo studio della neve e delle valanghe

Weissfluhjoch-Davos

Interner Bericht Nr. 712

Contribution on the skier stability index

Jürg Schweizer

Davos, 28. Dezember 1997

Interner Bericht Nr. 712

Contribution on the skier stability index

Der Institutsleiter:

W. Ammann

(W. Ammann)

Der Autor:

J. Schweizer

(J. Schweizer)

Davos, 28. Dezember 1997

Contents

1 Introduction

The present report compiles some aspects concerning the application of the skier stability index S' introduced by Föhn (1987). Jamieson (1995) contributed two important improvements: the consideration of the ski penetration and the independence of shear strength on normal load for persistent weak layers (such as surface hoar, depth hoar or faceted crystals). The main motivation was to check the hypothesis that the stability index decreases under natural loading conditions.

Before approaching the details the derivation of the skier stability index S' as presented by Föhn (1987) is briefly reviewed. The stability index in its general form as introduced by Roch (1966a) is a strength to load ratio, usually shear strength of the weak layer τ_s to shear stress in the weak layer due to the weight of the overlying slab τ_{xz} :

$$S = \frac{\tau_s}{\tau_{xz}} \tag{1}$$

A co-ordinate system with x-axis parallel to the snow surface (pointing down slope) and z-axis perpendicular to the slope pointing downward into the snow cover is used (Fig. 1).
Assuming a Mohr-Coulomb friction law with a friction coefficient μ (= $\tan\vartheta$, with angle of internal friction ϑ) and normal stress σ_z, the shear strength can be calculated from cohesion C measured with the shear frame (Roch, 1966a):

$$\tau_s = C + \tan\vartheta\,\sigma_z \tag{2}$$

Roch (1966b) derived the following empirical relation for the friction coefficient μ:

$$\tan\vartheta = \mu = 0.4 + 8\times10^{-5}\,C \tag{3}$$

For typical values of the cohesion (C = 500 ... 2000 Pa) the resulting friction angles ϑ are between 24° and 29°.
Usually the strength values measured are size corrected, since shear strength decreases with increasing frame area (for frame area smaller than about 0.5 m²). Correction factors for standard frame sizes of 0.01, 0.025 and 0.05 m² are 0.56, 0.65 and 0.71 respectively (Föhn, 1987; Jamieson, 1995). In the following it is assumed that all cohesion values are size corrected.
Therefore the stability index S can be given in detail as:

$$S = \frac{C + \left(0.4 + 8\times10^{-5}\,C\right)\rho g h\cos^2\psi}{\rho g h\cos\psi\sin\psi} \tag{4}$$

with slab density ρ , acceleration due to gravity g (9.81 ms^{-2}), slab thickness h (measured vertically) and slope angle ψ (Fig. 1).

Föhn (1987) introduced an additional term $\Delta\tau_{xz}$ in the denominator of eq. (1) to take into account the additional load by a skier. The skier stability index S' is therefore defined as:

$$S' = \frac{\tau_s}{\tau_{xz} + \Delta\tau_{xz}} \tag{5}$$

The skier's impact is assumed to act as a line load L (= 500 Nm^{-1}) on an elastic half space (Boussinesq's solution). Hence, the additional shear stress is given by:

$$\Delta\tau_{xz} = \frac{2L\cos\alpha\sin^2\alpha\sin(\alpha+\psi)}{\pi h\cos\psi} \tag{6}$$

where α is the angle from the snow cover to a point in the weak layer. Of particular interest to calculate the skier stability index is the peak shear stress (Fig. 1). The derivation of the angle for which the shear stress is largest (α_{max}) is given below in chapter 2.

30° : 282 | 1.0
35° : 299 | 1.06
40° : 319 | 1.13

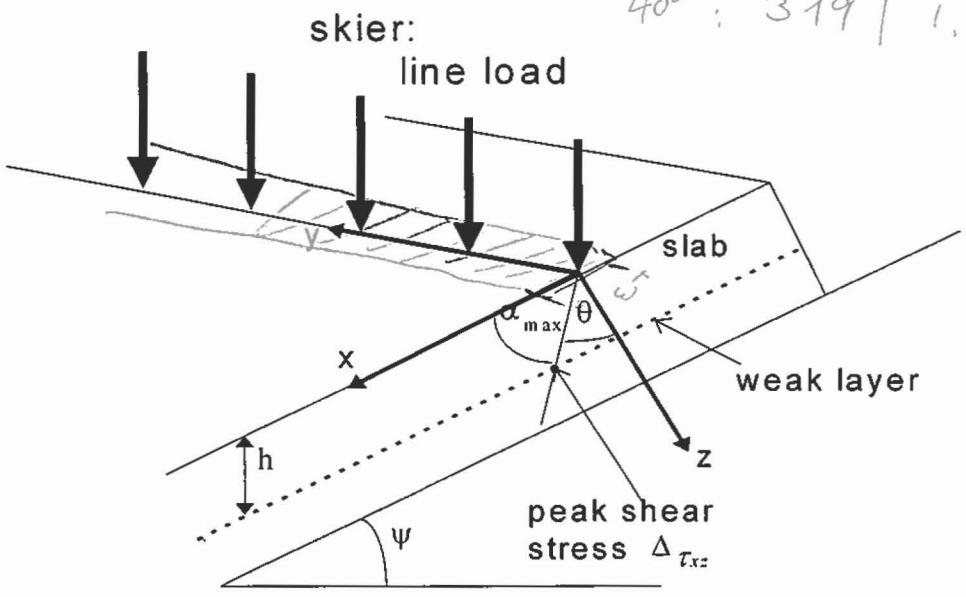

Fig. 1 Snow cover: co-ordinate system and notation

The additional shear stress by a skier hence decreases strongly with increasing depth ($\Delta\tau_{xz}$ ~ 1/h) (Fig. 2 and 3). Above the skier (up-slope) the shear stress is partly negative (Fig. 3 and 4) causing large stress gradients just below the skier (Fig. 5). For a skier on a typical avalanche slope (ψ = 38°), the peak shear stress $\Delta\tau_{xz}$ simplifies to 155/h Pa where the slab thickness h (measured vertically) is given in metres.

155.3251541

ψ = 38 α = 54.3438
max

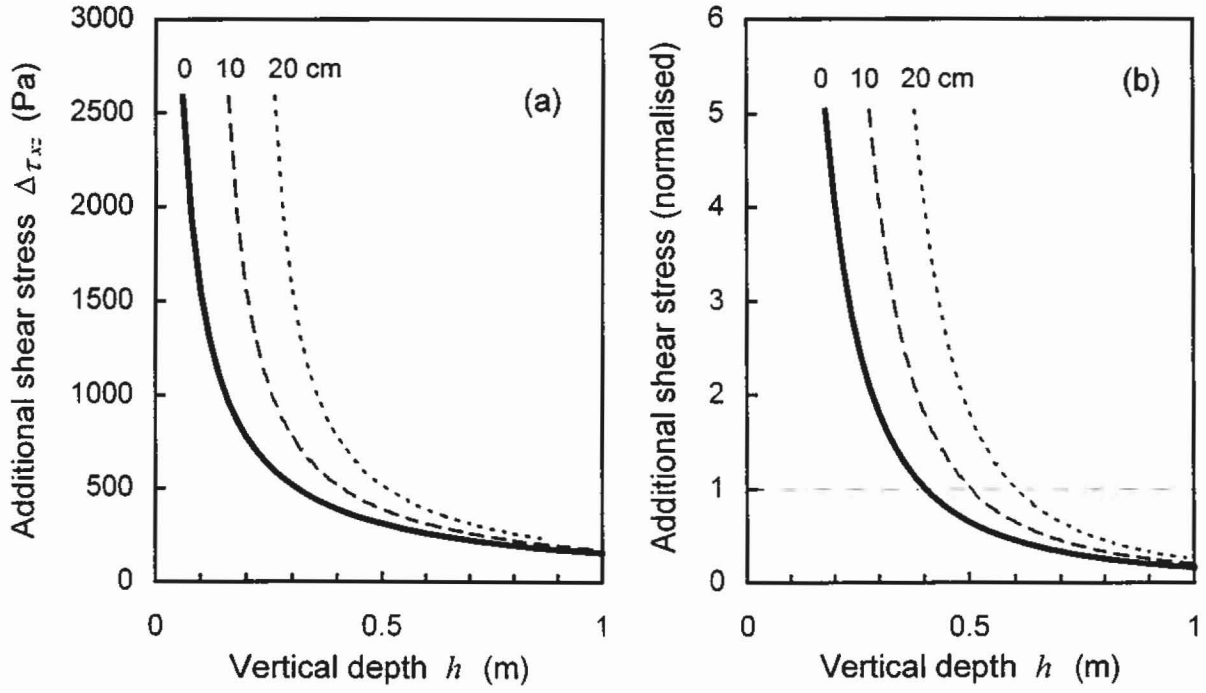

Fig. 2 Additional peak shear stress due to a skier (considered as line load) vs. depth: (a) for typical values (L = 500 Nm^{-1}, slope angle ψ = 38°), (b) normalised to the slab weight (density ρ = 200 kgm^{-3}). Dashed lines show effect of ski penetration depth, assumed to be 10 cm or 20 cm.

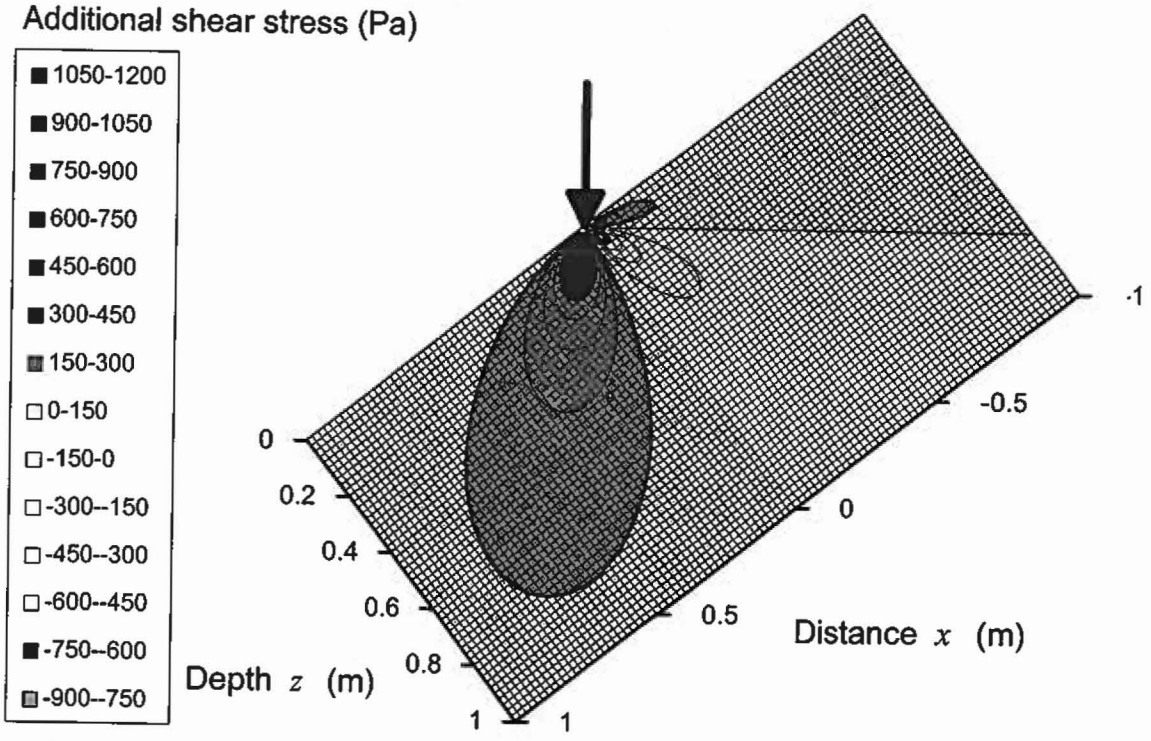

Fig. 3 Additional shear stress due to a skier (L = 500 Nm^{-1}, ψ = 38°) in a longitudinal section of the snow cover.

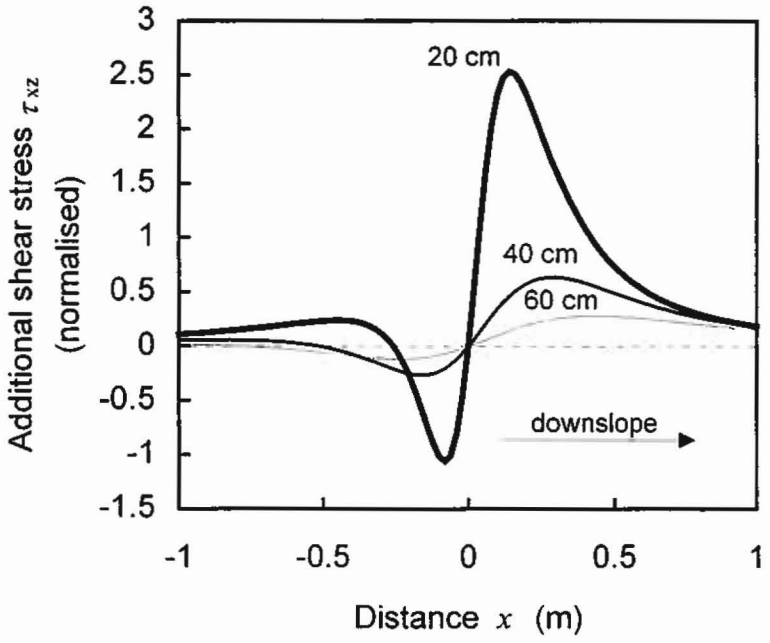

Fig. 4: Additional shear stress due to a skier (line load) in a longitudinal section of the snow cover, normalised to slab weight (ρ = 200 kgm^{-3}, ψ = 38°). Values for depth z = 20, 40 and 60 cm are given.

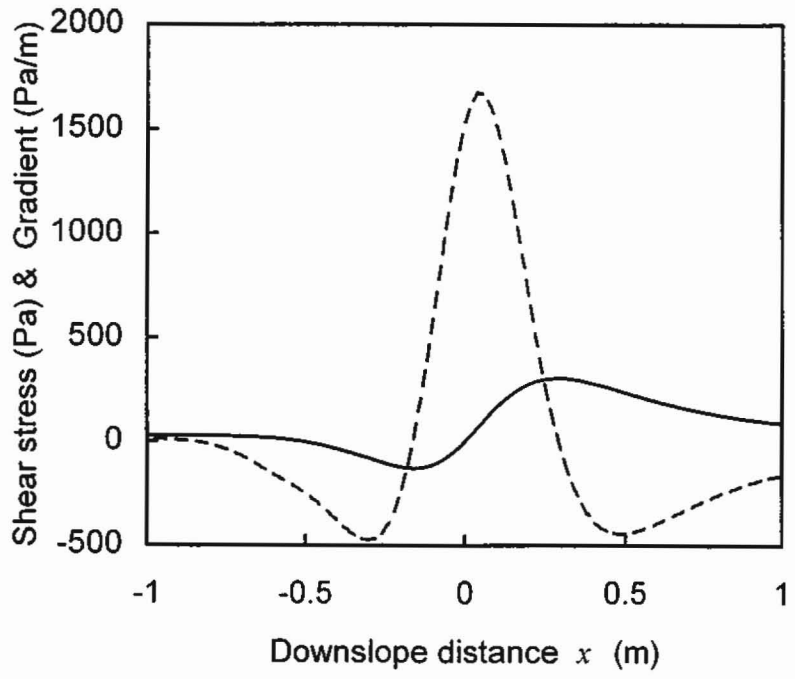

Fig. 5: Additional shear stress due to a skier (solid line) and its derivative, i.e. the stress gradient (dashed line), typical values, z = 40 cm.

2 Determination of α_{max}

The additional shear stress $\Delta\tau_{xz}$ depends on the angle α. To find the peak shear stress eq. 6 has to be differentiated with respect to α, and then the values of α (depending on slope angle ψ) have to be found such that the resulting equation equals zero:

$$\frac{d(\Delta\tau_{xz})}{d\alpha} = \frac{2L}{\pi\, h\cos\psi}\begin{pmatrix} 2\sin\alpha\cos^2\alpha\sin(\alpha+\psi) \\ -\sin^3\alpha\sin(\alpha+\psi) \\ +\sin^2\alpha\cos\alpha\cos(\alpha+\psi) \end{pmatrix} = 0 \qquad (7)$$

Eq. (7) can be solved numerically with a standard mathematical solver (e.g. MAPLE) for different values of the slope angle ψ. Results are given in Table 1. For slope angles of 0° and 90° values of α_{max} of 60° and 45° result, respectively. These two extreme cases correspond to the cases of a purely vertical and a horizontal line load in the flat terrain, respectively. (The values in Table 1 below differ from the ones originally given by Föhn (1987) since his eq. (5) still included the radius r that also depends on α .)

Table 1 Angle of maximum shear stress α_{max} for different values of the slope angle ψ.

slope angle: ψ (°)	angle of maximum shear stress: α_{max} (°)	slope angle: ψ (°)	angle of maximum shear stress: α_{max} (°)
25	56.20	36	54.63
26	56.06	37	54.49
27	55.91	38	54.34
28	55.77	39	54.20
29	55.63	40	54.06
30	55.49	41	53.91
31	55.34	42	53.77
32	55.20	43	53.62
33	55.06	44	53.47
34	54.92	45	53.33
35	54.77	50	52.28

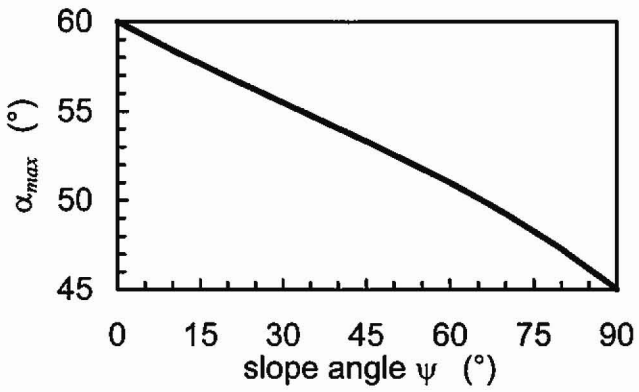

Fig. 5.1 Angle of maximum shear stress α_{max} vs. slope angle ψ.

3 Strip load

Of course, the skier stability index would be more correct if the skier would be approximated by a strip load rather than by a line load. However, as will be shown below, differences are small.

Following Das (1983) the shear stress due to a vertical strip load can be given as:

$$\Delta\tau_{xz} = \frac{p}{\pi}\left(\sin\varphi\sin(\varphi+2\theta)\right) \tag{8}$$

where p is the vertical load per unit area, and φ and θ are angles as defined in Figure 6.
Accordingly the shear stress due to a horizontal strip load can be given:

$$\Delta\tau_{xz} = \frac{q}{\pi}\left(\varphi-\sin\varphi\cos(\varphi+2\theta)\right) \tag{9}$$

where q is the horizontal load per unit area.

On a slope the skier's load can be given as the superposition of the component parallel and perpendicular to the slope:

$$\Delta\tau_{xz} = \frac{W\cos\psi}{2bl\pi}\left(\sin\varphi\sin(\varphi+2\theta)\right)+\frac{W\sin\psi}{2bl\pi}\left(\varphi-\sin\varphi\cos(\varphi+2\theta)\right) \tag{10}$$

where W is the weight of the skier (e.g. 850 N) and b and l are width and length of a ski respectively.

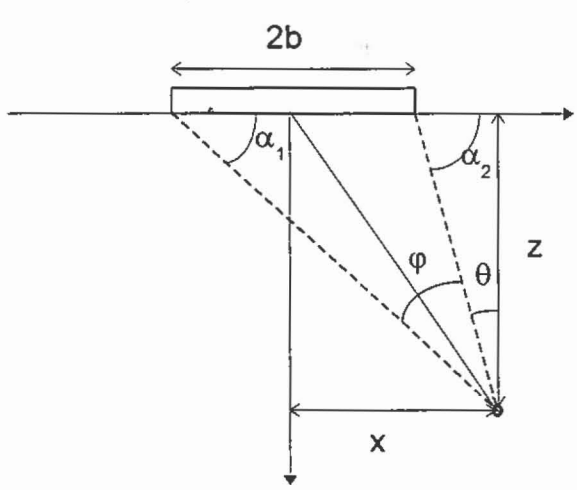

Fig. 6: Uniform loading on an infinite strip.

Using α_1 and α_2 (Fig. 6) an alternative formulation can be found:

$$\Delta\tau_{xz} = \frac{W\cos\psi}{2bl\pi}\left(\sin(\alpha_2-\alpha_1)\sin(\alpha_2+\alpha_1)\right) + \frac{W\sin\psi}{2bl\pi}\left((\alpha_2-\alpha_1)+\sin(\alpha_2-\alpha_1)\cos(\alpha_2+\alpha_1)\right)$$

This can be further simplified to get:

$$\Delta\tau_{xz} = -\frac{W\cos\psi}{2bl\pi}\frac{1}{2}\left(\cos 2\alpha_2-\cos 2\alpha_1\right) + \frac{W\sin\psi}{2bl\pi}\left((\alpha_2-\alpha_1)+\frac{1}{2}(\sin 2\alpha_2-\sin 2\alpha_1)\right) \quad (11)$$

The latter formulation is also given by Föhn (1987) who used the strip load calculation to approximate the additional shear stress due to a snowcat.

Fig. 7 shows the stress distribution in a longitudinal section of the snow cover. The main difference to the line load is that the shear stress at the top is well defined. However, under natural conditions the surface conditions are anyway unknown due to snow compaction and hence destruction of the surface layer. Using e.g. again the numerical values proposed by Föhn (1987) (skier weight W = 850 N, ski length l = 1.7 m, slope angle ψ = 38°) and a ski width b = 0.075 m the shear stress at the surface is about 2050 Pa. It is again strongly decreasing with increasing depth, and, except at the top, does not differ substantially from the line load solution (Fig. 8). The angle for which the additional shear stress is largest, is about 55° for the example given above (Fig. 7). It coincides well with the according value for the line load (Tab. 1). The stress distribution in a given depth along the slope does hardly change, too (Fig. 9).

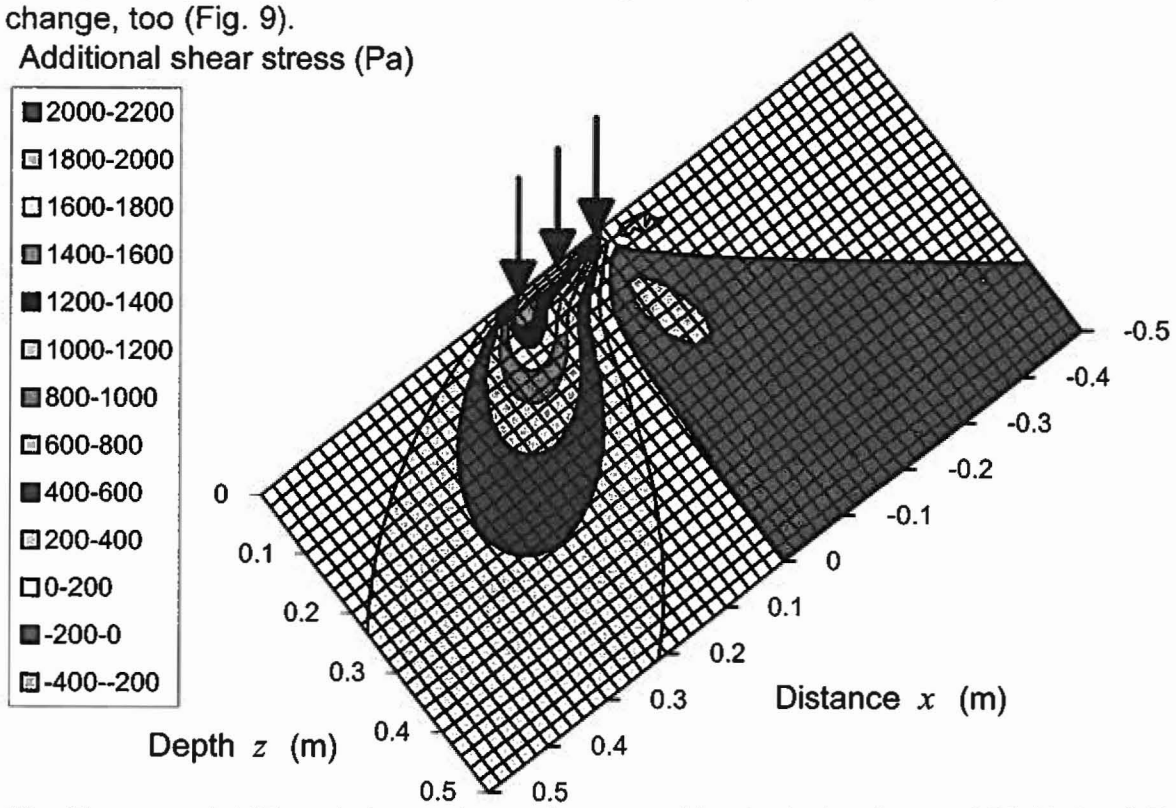

Fig. 7 Additional shear stress due to a skier (strip load: W = 850 N, l = 1.7 m, b = 0.075 and ψ = 38°) in a longitudinal section of the snow cover.

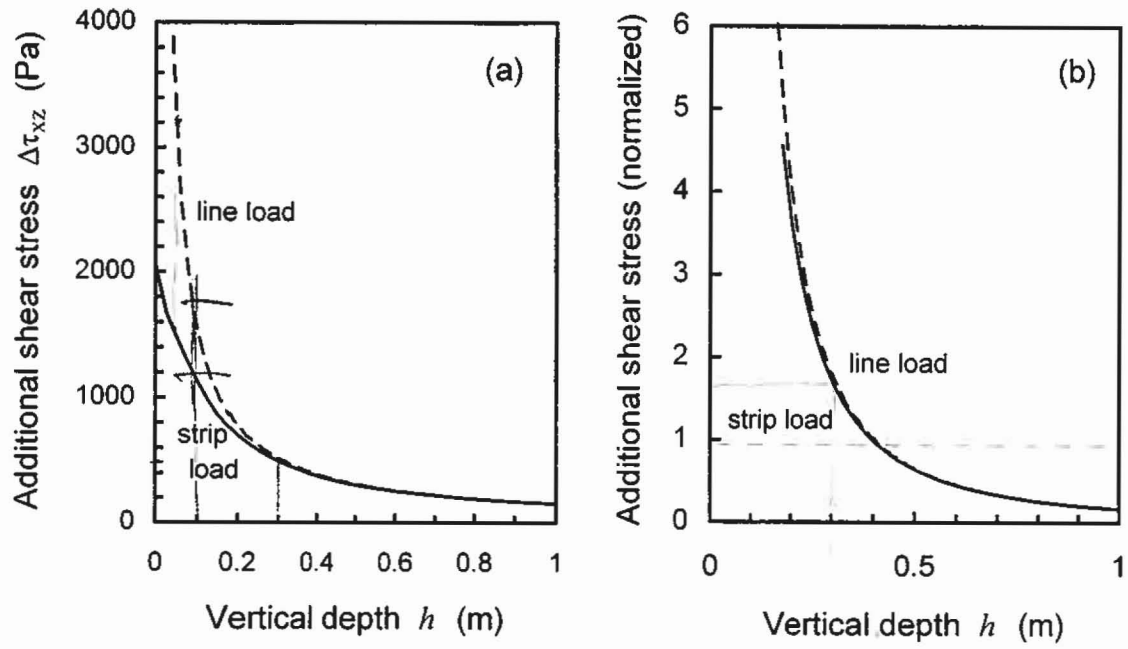

Fig. 8 Additional peak shear stress due to a skier vs. depth. Comparison between line and strip load. (a) for typical values (W = 850 N, l = 1.7 m, b = 0.075 m, slope angle ψ = 38°), (b) normalised to the slab weight (density ρ = 200 kgm^{-3}).

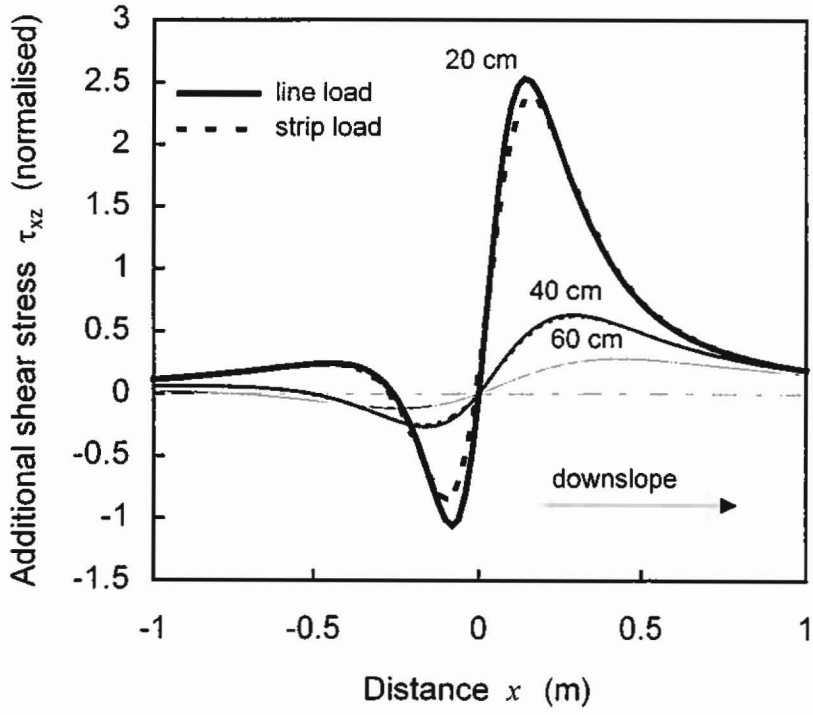

Fig. 9 Additional shear stress due to a skier in a longitudinal section of the snow cover, normalised to slab weight (density ρ = 200 kgm^{-3}). Comparison of line load (solid line) to strip load (dashed line) at depth z = 20, 40 and 60 cm.

Wider skis cause smaller stress values close to the surface but do not change the stress distribution deeper down (Fig. 10).

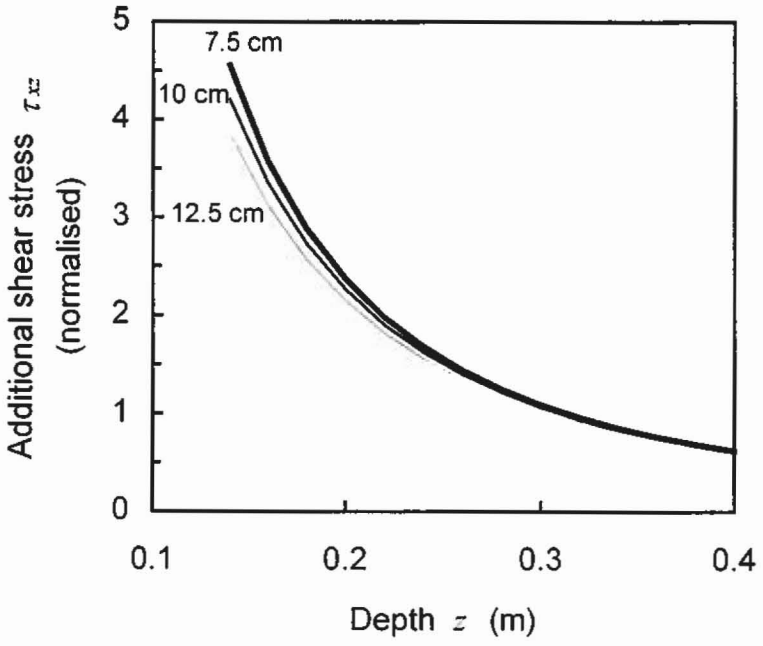

Fig. 10 Additional shear stress by a skier approximated by a strip load for different skier width (b = 7.5, 10 and 12.5 cm), normalised to shear stress due to slab weight.

4 Sensitivity on slope angle

In the following the sensitivity of the skier stability S' index is checked by differentiating with respect to the slope angle ψ. The skier is considered as a line load. Combining eq. 4, 5 and 6 the skier stability index S' can be given in detail as:

$$S' = \frac{C + (0.4 + 0.00008C)\rho g h \cos^2 \psi}{\rho g h \sin \psi \cos \psi + \frac{2L \cos \alpha \sin^2 \alpha}{\pi h} \cdot \frac{\sin(\alpha + \psi)}{\cos \psi}} \tag{12}$$

Using the following substitutions

$$A = \rho g h$$
$$B = 0.4 + 0.00008C$$
$$D = \frac{2L}{\pi h} \cos \alpha \sin^2 \alpha$$

eq. 12 simplifies to:

$$S' = \frac{C + BA \cos^2 \psi}{A \sin \psi \cos \psi + D \frac{\sin(\alpha + \psi)}{\cos \psi}}$$

Differentiation with respect to ψ gives:

$$\frac{dS'}{d\psi} = \frac{(-2BA \cos \psi \sin \psi)(A \sin \psi \cos \psi + D \frac{\sin(\alpha + \psi)}{\cos \psi})}{(A \sin \psi \cos \psi + D \frac{\sin(\alpha + \psi)}{\cos \psi})^2}$$
$$- \frac{(C + BA \cos^2 \psi)\left(A(\cos^2 \psi - \sin^2 \psi) + D(\frac{\cos(\alpha + \psi)\cos \psi + \sin(\alpha + \psi)\sin \psi}{\cos^2 \psi}) \right)}{(A \sin \psi \cos \psi + D \frac{\sin(\alpha + \psi)}{\cos \psi})^2} \tag{13}$$

Accordingly dS'/dψ < 0 for any physically reasonable values, i.e. the skier stability index is always decreasing with increasing slope angle as illustrated in Figs. 11-14. Fig. 11 and 12 show that slope sensitivity is more pronounced for higher values of the cohesion (or shear stress) and for deeper layers. In addition the gradient itself varies more for deeper layers than for shallow layers (Fig. 12 and 13), i.e. strongly

increases with slope angle. For shallow layers the derivative of the skier stability index with respect to the slope angle only slightly increases.
For deeper layers the density has some influence. The lower the density the larger the slope effect. For shallow layers the layer density is not important (Fig.13).

Considering the effect of ski penetration (Fig. 14) shows that the larger the ski penetration the smaller the slope effect. Similarly for the effect of the frictional part of the shear strength. Jamieson (1995) showed that the shear strength of persistent weak layers does not depend on normal load. If the shear strength is not corrected for normal load the slope effect decreases (Fig. 14). So considering ski penetration and pressure insensitivity, both contributing to more realistic conditions, results in lower slope sensitivity.

For typical numerical values (as above) the gradient (derivative of the skier stability index with respect to the slope angle) varies between about -2.5 and -1. This means the skier stability index decreases by about 0.65 to 0.26 for an increase of the slope angle from e.g. 30° to 45°. Using the relation Jamieson (1995) derived (eq. 7.1, p. 177-178) between the skier stability index and the rutschblock score this corresponds to a decrease of 1 to 2 rutschblock scores per 15° increase in slope angle.

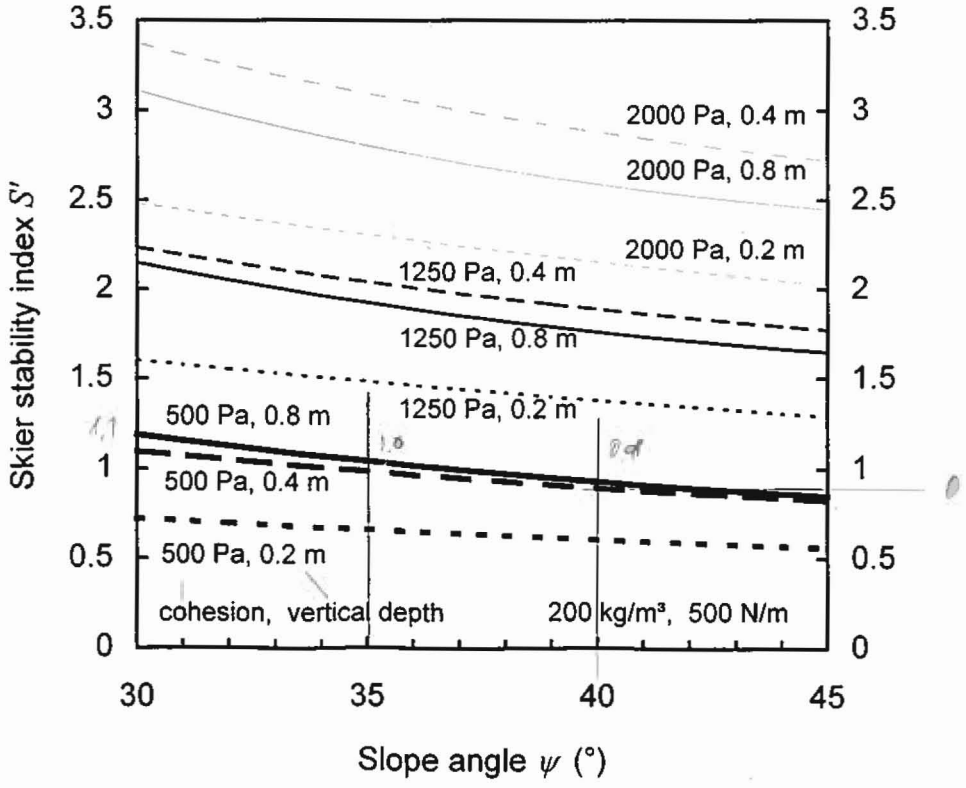

Fig. 11 Effect of slope angle on skier stability index for some typical values of the cohesion, and for three values of vertical layer depth (0.2, 0.4 and 0.8 m). Other numerical values used are slab density: 200 kg/m³, and skier represented as line load: 500 N/m.

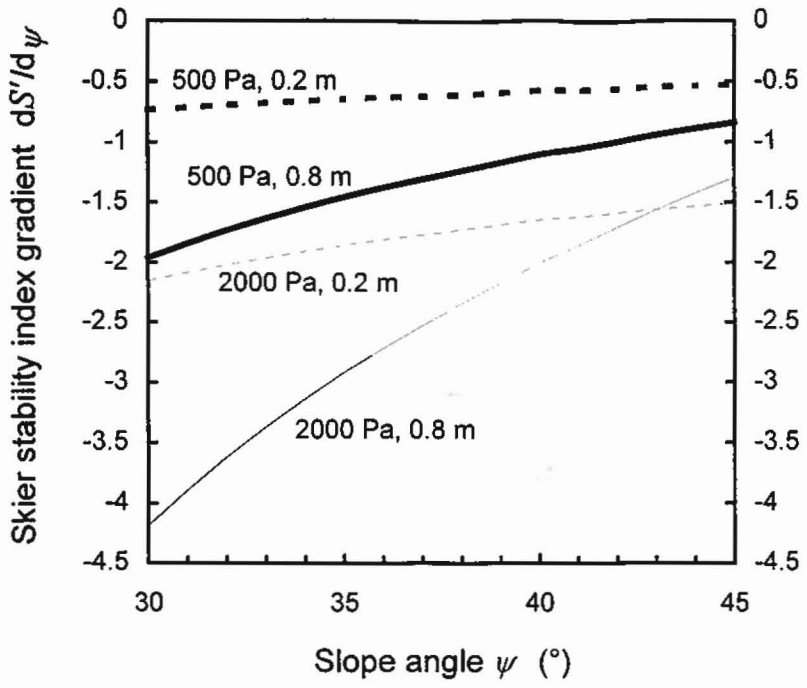

Fig. 12 Effect of slope angle on the derivative of the skier stability index with respect to slope angle ($dS'/d\psi$) for a low and a high value of the cohesion (500, 2000 Pa), each for a shallow (0.2 m) and a deep (0.8 m) slab.

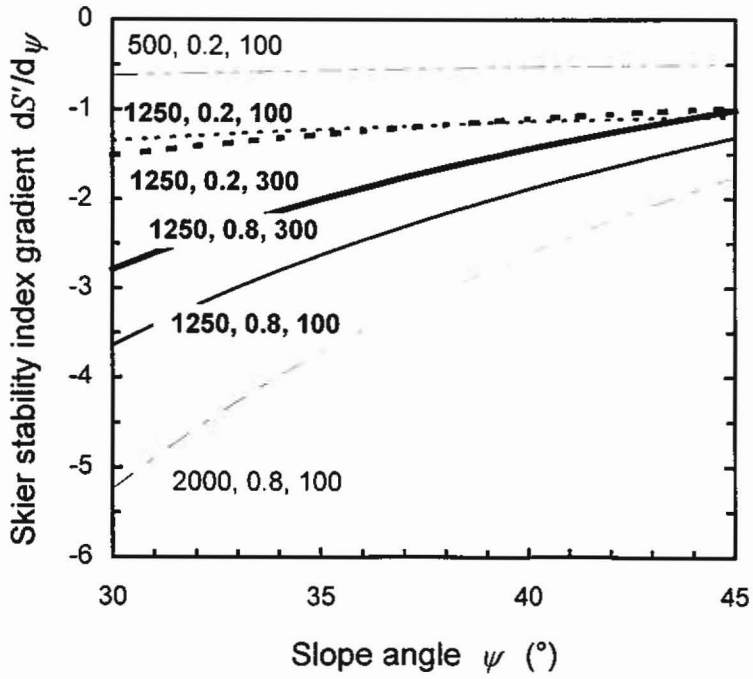

Fig. 13 Effect of slope angle and density on $dS'/d\psi$. Curves are shown for an intermediate value of the cohesion (1250 Pa) and two values of density (100 and 300 kgm^{-3}), each for a shallow and a deep slab (0.2 m and 0.8 m). To illustrate variability two extreme cases are also given, represented by the uppermost curve (cohesion: 500 Pa, density: 100 kg/m^3 and layer depth: 0.2 m) and the lowest curve (cohesion: 2000 Pa, density: 100 kgm^{-3}, and layer depth: 0.8 m).

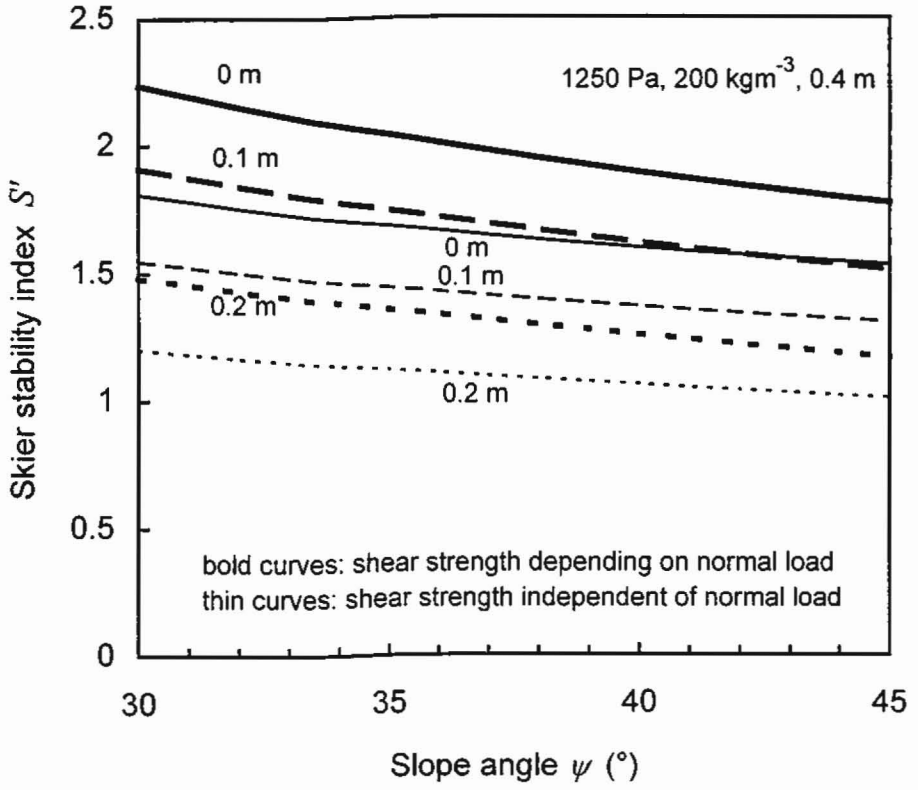

Fig. 14 Effect of slope angle, penetration depth and pressure sensitivity of shear strength on skier stability index for one typical example (cohesion 1250 Pa, density: 200 kgm^{-3}, layer depth: 0.4 m). Bold curves show effect of penetration depth (0.1 and 0.2 m) for shear strength depending on normal load, thin curves for shear strength independent of normal load.

5 Sensitivity on loading

In the following the sensitivity of the stability index on loading is evaluated. The question is, does the stability index increase or decrease under natural loading conditions. Additional artificial loading always decreases stability.
The additional natural load results from a snowfall, i.e. an additional snow layer is added. Accordingly normal and shear stress increase, whereas the skier stress decreases. It is assumed that the new snow layer has the same density as the layer below. So in all cases slab density is uniform. This assumption is not restrictive. Furthermore it is assumed that the weak layer properties are unchanged, too. In reality the weak layer in general slowly gains strength after natural loading. Therefore the above question can be answered by simply differentiate the stability index with respect to the layer depth (or slab thickness) h, and analysing the resulting expression.

First the natural stability index (eq. 4) is considered:

$$\frac{dS}{dh} = \frac{d}{dh}\left(\frac{C+(0.4+0.00008C)\rho g h\cos^2\psi}{\rho g h\cos\psi\sin\psi} \right) = -\frac{C}{\rho g\sin\psi\cos\psi}\cdot\frac{1}{h^2} \qquad (14)$$

The first factor on the right hand side (including cohesion, density and slope angle) is always positive. Accordingly the natural stability index S always decreases with increasing slab depth, independent of cohesion, density and slope angle.

Accordingly for the skier stability index S' as given in eq. (12):

$$S' = \frac{C+(0.4+0.00008C)\rho g h\cos^2\psi}{\rho g h\sin\psi\cos\psi + \frac{2L\cos\alpha\sin^2\alpha}{\pi h}\cdot\frac{\sin(\alpha+\psi)}{\cos\psi}}$$

Using the following substitutions

$$A = \rho g\cos\psi$$
$$B = 0.4+0.00008C$$
$$D = \frac{2L}{\pi}\,\frac{\cos\alpha\sin^2\alpha\sin(\alpha+\psi)}{\cos\psi}$$

the above expression simplifies to:

$$S' = \frac{C+BAh\cos\psi}{Ah\sin\psi+\frac{D}{h}} = \frac{Ch+BAh^2\cos\psi}{Ah^2\sin\psi+D}$$

Differentiation with respect to h gives:

$$\frac{dS'}{dh} = \frac{(C + 2BAh\cos\psi)(D + Ah^2\sin\psi) - (Ch + BAh^2\cos\psi)(2Ah\sin\psi)}{(D + Ah^2\sin\psi)^2} \qquad (15)$$

From eq.(5) the skier stability index increases under natural loading if

$$\frac{dS'}{dh} > 0$$

and the skier stability index decreases under natural loading if the derivative

$$\frac{dS'}{dh} < 0 \quad .$$

The derivative of S' with respect to h is analysed to find any zeros that correspond to extrema of the skier stability index.
The denominator is always positive for any value of h if the slope angle is not zero. To find zeros the numerator is set to zero and solutions for h are seeked:

$$(C + 2BAh\cos\psi)(D + Ah^2\sin\psi) - (Ch + BAh^2\cos\psi)(2Ah\sin\psi) = 0$$

The following quadratic equation results:

$$CD + 2ABDh\cos\psi - ACh^2\sin\psi = 0$$

with the following two solutions:

$$h_{1,2} = \frac{-2ABD\cos\psi \pm \sqrt{(2ABD\cos\psi)^2 + 4AC^2D\sin\psi}}{-2AC\sin\psi}$$

One of which is always negative. So the only physical solution is the slab depth h^* for which the skier stability index is largest:

$$h^* = \frac{-2ABD\cos\psi - \sqrt{(2ABD\cos\psi)^2 + 4AC^2D\sin\psi}}{-2AC\sin\psi} \quad . \qquad (16)$$

For values smaller or larger than h^* the skier stability index decreases.

The above derivation is in the following illustrated with some numerical examples. In addition the effects of normal load on shear strength and of ski penetration are studied.

Fig. 15 summarises some of the basic features. It shows the decreasing natural stability for increasing depth of weak layer, and the typical course of the skier stability index with increasing depth, showing a maximum. In other words the skier stability index increases with increasing natural loading for initially shallow to intermediate layer thickness. This rather surprising result is not new (cf. Schweizer, 1991, Fig. 1) but has never been discussed. It results from the fact that the skier shear stress decreases more strongly than the shear stress due to the slab weight increases, and in addition the shear strength also slightly increases due to its normal stress dependence. The steeper the slope and the smaller the cohesion the smaller the increase of the skier stability index.

The layer thickness for which the skier stability index shows a maximum value (eq. 16), the depth of maximal stability h^*, depends on cohesion, slab density and slope angle. It increases with decreasing cohesion, decreasing slope angle and increasing density (Fig. 16 and 17). The effect of slope angle is minor compared to the effects of cohesion and density.

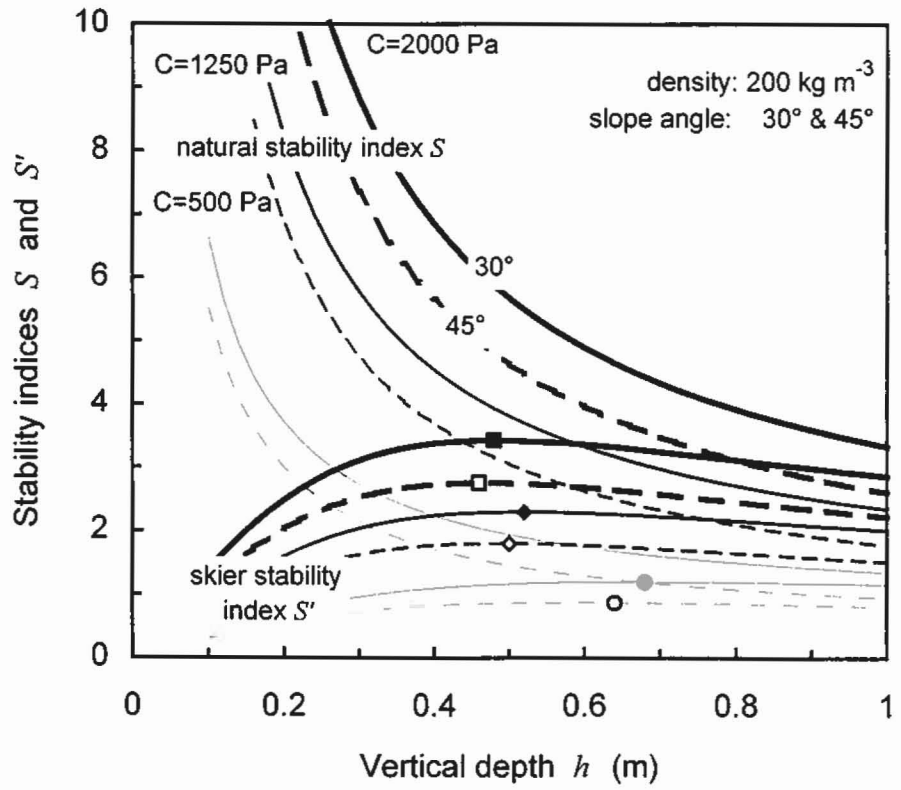

Fig. 15 Natural and skier stability index vs. layer depth (or slab thickness) for different values of the cohesion (500, 1250 and 2000 Pa) and for two slope angles: 30° (solid) and 45° (dashed lines) that suggest the limits. The symbols indicate the maxima for the skier stability index. Slab density is 200 kgm^{-3}.

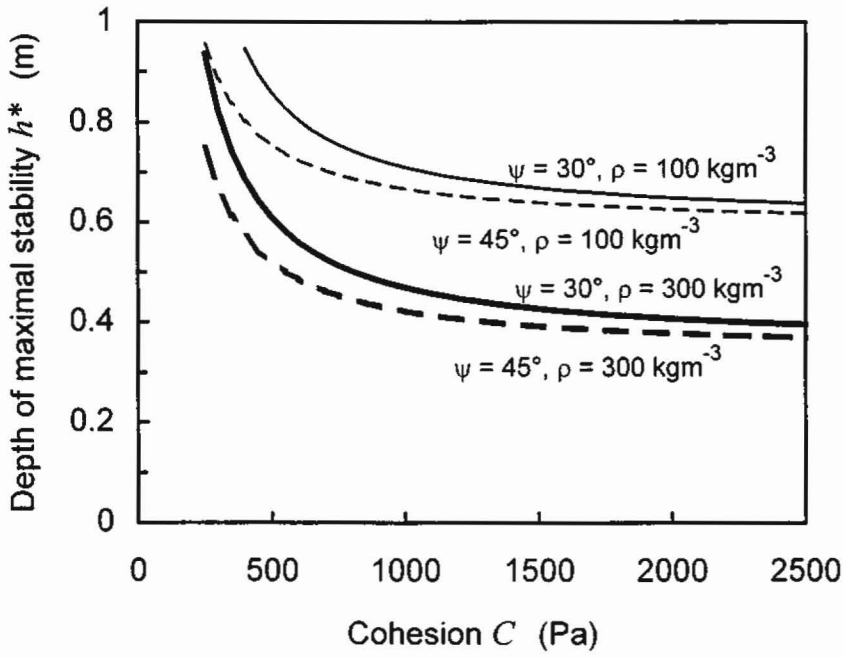

Fig. 16 Depth of maximal stability h^* (the layer thickness for which the skier stability index shows a maximum value) vs. cohesion for two different slope angles (30°, 45°) and densities (100, 300 kgm^{-3}) that comprise the range of realistic values.

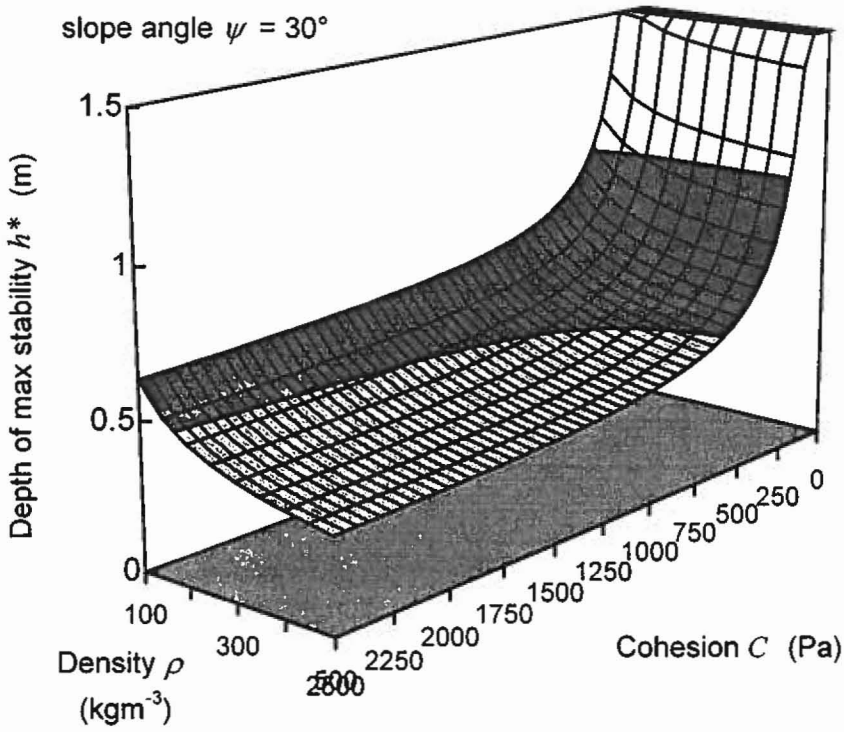

Fig. 17 Depth of maximal stability h^* (the layer thickness for which the skier stability index shows a maximum value) vs. cohesion and density. Slope angle is 30°.

From the above analysis it seems clear that for any realistic values the skier stability index will show a maximum with increasing layer depth. However, for most realistic cases the flat course of the curves implies that the skier stability index shows little change, e.g. if the layer thickness increases from 40 to 60 cm.

Finally, in the following the effects of ski penetration depth and normal stress dependence of shear strength is studied. The question is how these two effects influence the above described features.
In Fig. 18 both effects are shown for some numerical values. In general the skier stability index still shows a maximum value. Considering the penetration depth results in larger values of the depth of maximal stability h^*, whereas the pressure independence of the shear strength leads to smaller values of h^*. Both effects of course decrease the skier stability index.
As can be seen in Fig. 18 for realistic conditions (i.e. no pressure dependence, increasing ski penetration with natural loading) the skier stability index decreases if e.g. the layer thickness increases from 40 to 60 cm, and consequently the penetration depth also increases from e.g. 10 to 20 cm.

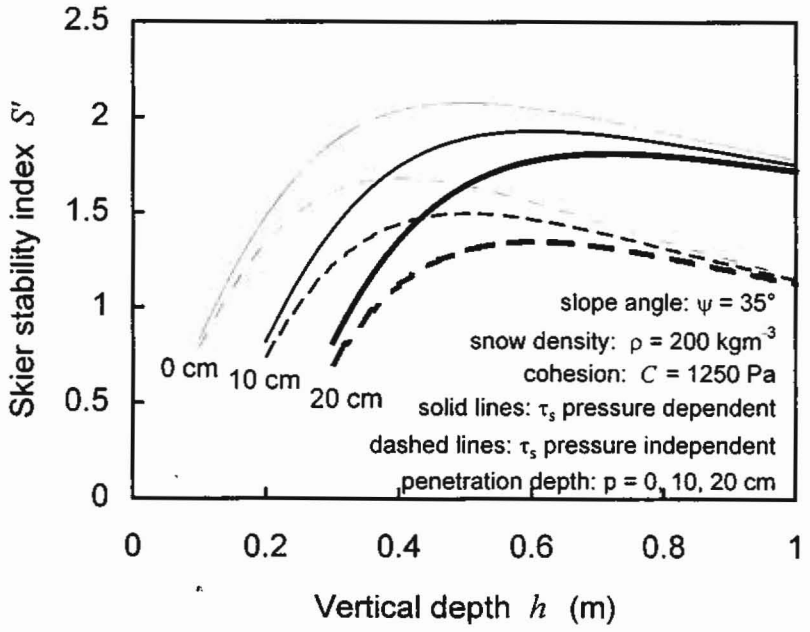

Fig. 18 Skier stability index S' vs. vertical depth h showing the effects of ski penetration (0, 10 and 20 cm) and normal stress on shear strength. Solid lines are shown for shear strength including normal stress, dashed lines without consideration of normal stress. Typical values for cohesion and density are assumed (1250 Pa, 200 kgm^{-3}). Slope angle is 35°.

If the shear strength does not depend on normal stress the skier stability index can be given as:

$$S' = \frac{C}{\rho g h \cos\psi \sin\psi + \frac{2L}{\pi} \cdot \frac{\cos\alpha \sin^2\alpha \sin(\alpha+\psi)}{h\cos\psi}}$$

Using the following substitutions

$$E = \rho g \cos\psi \sin\psi$$

$$D = \frac{2L}{\pi} \frac{\cos\alpha \sin^2\alpha \sin(\alpha+\psi)}{\cos\psi}$$

the above expression simplifies to:

$$S' = \frac{C}{Eh + \frac{D}{h}} = \frac{Ch}{Eh^2 + D}$$

Differentiation with respect to h gives:

$$\frac{dS'}{dh} = \frac{C(Eh^2 + D) - Ch(2Eh)}{(Eh^2 + D)^2}$$

Again we check for any maxima:

$$CEh^2 + CD - 2CEh^2 = 0$$

Thus the depth of maximal stability h_n* can be derived to:

$$h_n{}^* = \frac{D}{E} = \sqrt{\frac{2L\cos\alpha \sin^2\alpha \sin(\alpha+\psi)}{\pi\rho g \cos^2\psi \sin\psi}} \quad . \tag{17}$$

The depth of maximal stability hence becomes independent of the shear strength, if the shear strength does not depend on normal stress and is in general smaller than if the shear strength depends on normal stress (Fig. 19). Accordingly h_n* primarily depends on density. The slope effect is very minor (Fig. 19).

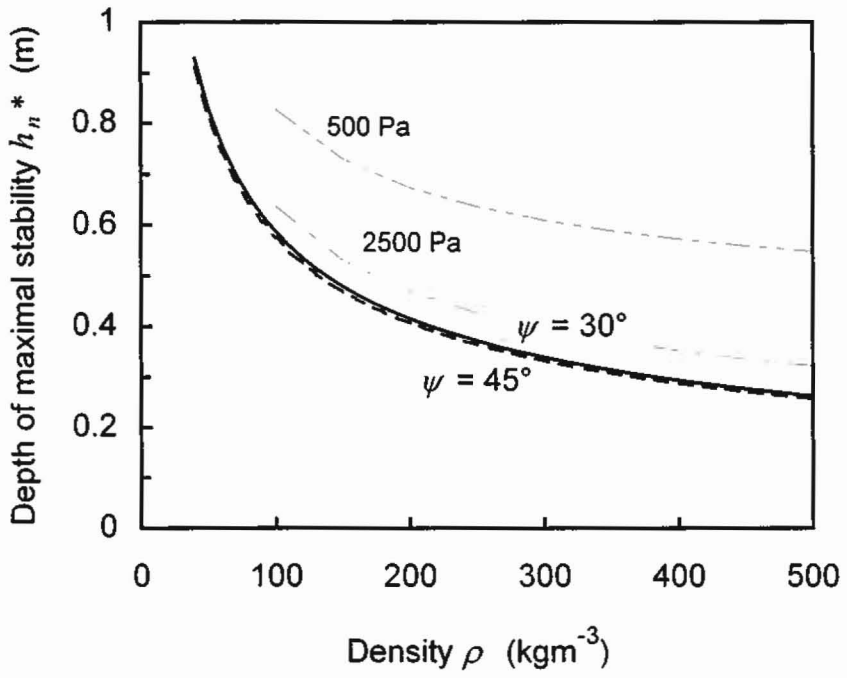

Fig. 19 Depth of maximal stability h_n* vs. density for two different slope angles: 30° (solid line) and 45° (dashed line). Shear strength is independent of normal stress. Therefore h_n* becomes independent of shear strength (or cohesion). h* is larger for any realistic value of the cohesion than h_n* which is illustrated by the two examples also given (thin dash-point lines).

If in addition to normal stress independence of shear strength, the ski penetration depth is included, the skier stability index can be given as:

$$S' = \frac{C}{\rho g h \cos\psi \sin\psi + \frac{2L}{\pi} \cdot \frac{\cos\alpha \sin^2\alpha \sin(\alpha+\psi)}{(h-p)\cos\psi}}$$

Using again the following substitutions

$$E = \rho g \cos\psi \sin\psi$$

$$D = \frac{2L}{\pi} \frac{\cos\alpha \sin^2\alpha \sin(\alpha+\psi)}{\cos\psi}$$

the above expression simplifies to:

$$S' = \frac{C}{Eh + \frac{D}{h-p}} = \frac{C(h-p)}{Eh(h-p)+D}$$

Differentiation with respect to h gives:

$$\frac{dS'}{dh} = \frac{C(Eh^2 - Ehp + D) - C(h - p)(2Eh - Ep)}{(Eh(h - p) + D)^2}$$

Again we check for any maxima, setting the numerator to zero:

$$-CEh^2 + 2CEhp + CD - CEp^2 = 0$$

Thus the depth of maximal stability h_{np}* can be derived to:

$$h_{np}\,* = \frac{-2Ep - \sqrt{4E^2p^2 + 4E(D - Ep^2)}}{-2E} \quad . \tag{18}$$

Again the depth of maximal stability is independent of the shear strength (or cohesion), and if the penetration depth p is set to zero, eq. (17) results.

As already could be seen in Fig. 18 considering the ski penetration increases the depth of maximal stability (Fig. 20). Comparing Figs. 19 and 20 shows that the two effects considered (normal stress dependence of shear strength and ski penetration) act in opposite direction.

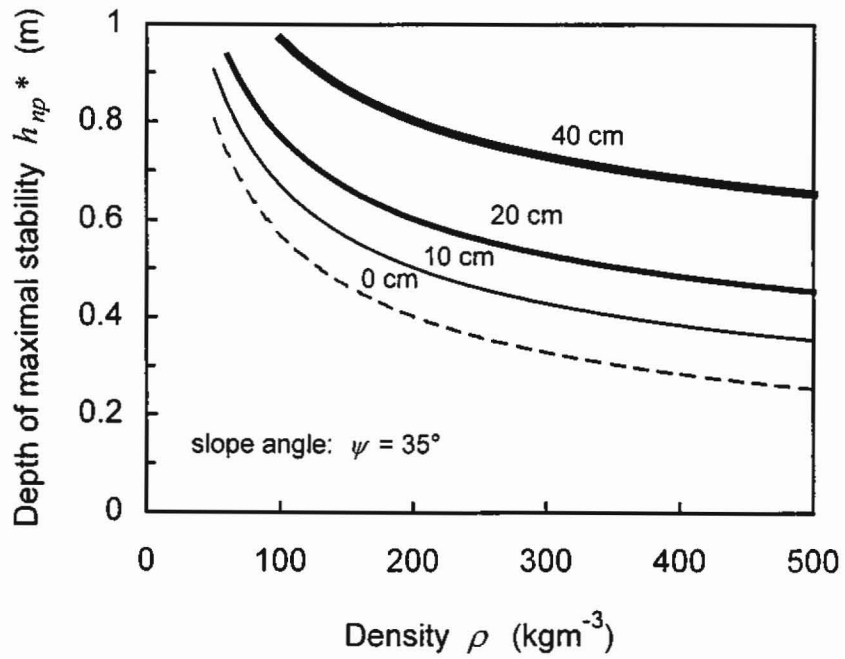

Fig. 20 Depth of maximal stability h_{np}* vs. density for different values of the ski penetration depth: 10, 20 and 40 cm (solid lines). For comparison the curve that does not include ski penetration is also given (dashed line). Slope angle is 35°.

As supposed above for most realistic cases the skier stability index shows little change. It slightly increases, remains more or less unchanged or even decreases. As realistic conditions we assume: shear strength is independent of normal stress, typical values are taken: 1250 Pa (Föhn, 1993), ski penetration is typically 10 to 20 cm for initial slab height of 30 to 60 cm, slope angle is 35°, initial slab density is 200 kgm^{-3}. Natural loading means that a new snow layer of thickness h' is added with density ρ' of 100 kgm^{-3} and a penetration depth of e.g. half the new layer thickness ($h'/2$). Accordingly the skier stability index can be given as:

$$S' = \frac{C}{(\rho h + \rho' h')g\cos\psi\sin\psi + \frac{2L}{\pi}\cdot\frac{\cos\alpha\sin^2\alpha\sin(\alpha+\psi)}{(h-p+h'/2)\cos\psi}}$$

The results are given in Fig. 21. It shows that except for the cases with small effective depth (h-$p \leq 20$ cm) the skier stability usually slightly decreases for natural loading of at least about 20 cm.

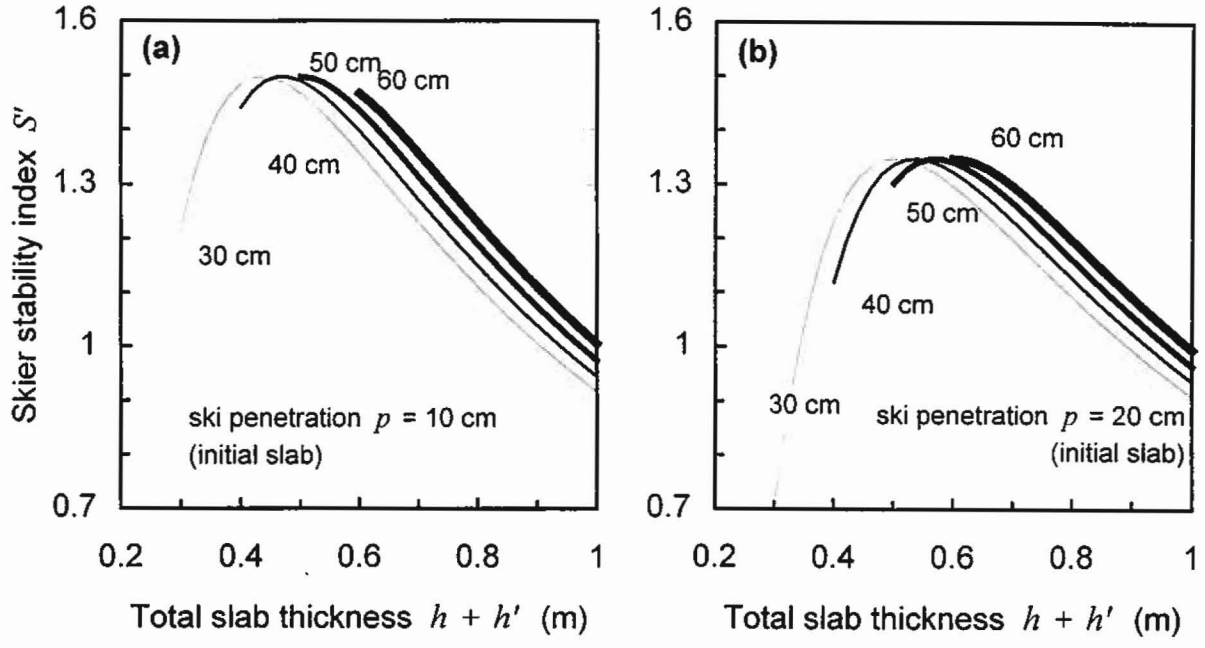

Fig. 21 Skier stability index S' vs. total slab thickness $h+h'$ for natural loading conditions with initial slab thickness of 30, 40, 50 and 60 cm. New snow density: 100 kgm^{-3}, and ski penetration half of the new snow depth. Initial layer density is 200 kgm^{-3}, cohesion is 1250 Pa, slope angle is 35° and ski penetration is (a) 10 cm and (b) 20 cm.

6 Conclusions

Some new aspects of the skier stability index have been studied and described. All of them corroborate the general concept introduced by Föhn (1987).

The skier stress strongly decreases with depth regardless whether the skier is modelled as line or strip load. Although the strip load is more realistic there is hardly any difference between the two formulations. The angle of maximum additional skier shear stress was re-calculated and is about 55°, again independent of the load model (line or strip).

The change of the skier stability index on a change of the slope angle is rather small. It is of secondary importance, e.g. a change of slope angle from 33° to 38° decreases the skier stability index S' by less than 10% using typical values (h = 0.4 m, ρ = 200 kgm^{-3}, C = 500 to 1250 Pa). Following a derivation by Jamieson (1995) it is suggested that an increase of the slope angle from 30° to 45° corresponds to a decrease of about 1 to 2 rutschblock scores.

Under natural loading conditions (new snow) the stability index S obviously always decreases. However, the skier stability index S' may either decrease or increase. In fact the skier stability index shows a maximum under all conditions, regardless whether ski penetration or the dependence of shear strength on normal stress is considered or not. The maximum is typically found for a vertical layer depth of 30 to 70 cm. The maximum results from the fact that under natural loading the skier stress more strongly decreases with increasing layer depth than the natural shear stress increases. This holds in particular for shallow and intermediate layer depth. But, as the course of the curve describing the skier stability index vs. layer depth is rather flat, the increase (or decrease) of the skier stability index is rather small. In addition, there exist many realistic cases, when there is hardly any change or the index decreases. This is the case if the initial depth is close to the maximum. In general, for shallow layers (considering ski penetration) skier stability first increases, then decreases under natural loading. For intermediate to deep slabs it generally decreases under natural loading.

Finally, since the skier stability index once again proved to be a valuable concept, which is also confirmed by field measurements (Schweizer et al., 1995; Camponovo and Schweizer, 1997), it seems reasonable to further improve it. A major step forward would be to include slab properties, since numerical simulations using the finite element method (Schweizer, 1993) and field measurements (Schweizer et al., 1995) have shown that the type of layering is crucial for skier triggering.

* slope angle influences: snow pack properties by increasing destructive metamorphism due to increased shading,

\+ steeper slope means shorter critical length needed for fracture propagation.

References

Camponovo, C. and J. Schweizer. 1997. Measurements on skier triggering. *Proceedings International Snow Science Workshop 1996*, Banff, Alberta, Canada, 6-10 October 1996, 100-103.

Das, B.M. 1983. *Advanced soil mechanics.* McGraw-Hill, New York, 511 pp.

Föhn, P.M.B. 1987. The stability index and various triggering mechanism. *IAHS Publication*, 162, 195-214.

Föhn, P.M.B. 1993. Characteristics of weak snow layers or interfaces. *Proceedings International Snow Science Workshop 1992*, Breckenridge, Colorado, U.S.A., 4-8 October 1992, 160-170.

Jamieson, J.B. 1995. *Avalanche prediction for persistent snow slabs.* Ph.D. Thesis. University of Calgary, Calgary, Alberta, Canada, 258 pp.

Roch, A. 1966a. Les déclenchements d'avalanches. *AIHS Publication*, 69, 182-195.

Roch, A. 1966b. Les variations de la résistance de la neige. *AIHS Publication*, 69, 86-99.

Schweizer, J. 1991. Dry snow slab avalanches triggered by skiers. *Proceedings International Snow Science Workshop 1990*, Bigfork, Montana, U.S.A., 9-13 October 1990, 307-309.

Schweizer, J. 1993. The influence of the layered character of the snow cover on the triggering of slab avalanches. *Ann. Glaciol.*, 18, 193-198.

Schweizer, J., C. Camponovo, C. Fierz and P.M.B. Föhn. 1995. Skier triggered slab avalanche release - some practical implications. In: *Proc. Int. Symposium: Sciences and mountain - The contribution of scientific research to snow, ice and avalanche safety*, ANENA, Chamonix, May 30 - June 3, 1995, 309-315.